

## **Supplemental Material to:**

**Siva Charan Devanaboyina, Sandra M Lynch,  
Raimund J Ober, Sripad Ram, Dongyoung Kim,  
Alberto Puig-Canto, Shannon Breen, Srinath  
Kasturirangan, Susan Fowler, Li Peng, Helen  
Zhong, Lutz Jermutus, Herren Wu, Carl Webster,  
E Sally Ward, and Changshou Gao**

**The effect of pH dependence of antibody-antigen  
interactions on subcellular trafficking dynamics**

**mAbs 2013; 5(6)**

**<http://dx.doi.org/10.4161/mabs.26389>**

**<http://www.landesbioscience.com/journals/mabs/article/26389/>**

## Supplementary Information

### SI Materials & Methods

*Selection and production of anti-IL-6 scFvs:* Anti-IL-6 antibodies were isolated from a large phage antibody library displaying human single chain Fvs (scFvs) on filamentous phage,<sup>1, 2</sup> using repeated selection cycles on recombinant human IL-6 as described previously.<sup>3</sup> ScFvs were purified from *Escherichia coli* periplasmic extracts using immobilized metal affinity chromatography.<sup>4</sup> Twenty-two scFvs from the selections were analyzed for the pH dependence of their binding to IL-6 by BIAcore.

*Histidine scanning mutagenesis:* For the targeted introduction of histidine residues in the VH and VL domain genes of the 0218, CDR3s were identified by the definition of Kabat.<sup>5</sup> Each codon of CDR3 of the VH and VL domains was systematically replaced by a histidine codon. The mutated genes were synthesized by GeneArt (Life Technologies, Grand Island, NY) and cloned into plasmids containing the human IgG1/kappa constant domains. Full length human IgG1 molecules were expressed in mammalian cells and purified using protein A-Sepharose. Concentrations of purified antibodies were determined using the BCA assay (Catalog no. 23225, Thermo Scientific, IL) and/or spectrophotometrically (A280 nm) as described previously.<sup>3</sup>

*Labeling of IL-6 and antibodies:* IL-6 (Catalog no. 206-IL/CF, R&D Systems, Minneapolis, MN) was labeled with Alexa Fluor-555 carboxylic acid, succinimidyl ester (Catalog no. A20009, Invitrogen, Grand Island, NY) with a degree of labeling (DOL) of 0.8 dye molecules per IL-6 molecule. Antibodies were labeled with Atto-647N NHS ester (Catalog no. 18373, Sigma-Aldrich, St. Louis, MO). The degrees of labeling for antibodies were 1, 1.3 or 1.4 dye molecules

per molecule of 0222, 0218 and VH4, respectively. Following the labeling reactions, IL-6 and antibodies were dialyzed against phosphate buffered saline, pH 7.4.

*Affinity determination and competition assays using surface plasmon resonance:* Equilibrium binding affinities of the interactions between IL-6 and anti-IL-6 antibodies or single chain Fvs (scFvs) were determined using surface plasmon resonance (BIAcore 2000) and previously described methods.<sup>6</sup> IL-6, antibodies or scFv fragments were coupled to flow cells of CM5 chips through amine coupling chemistry to a density of ~ 1500 RU for IL-6, or ~ 1000 RU for scFvs and full-length antibodies. To avoid avidity effects, IL-6 was used as analyte only for analyses of IgGs, whereas binding studies for scFvs were performed using IL-6 as both analyte and ligand. Reference flow cells were coupled with coupling buffer only during the coupling reaction. Analyte (IL-6 or scFv) was injected over the flow cells at a rate of 10  $\mu$ l/min at different concentrations, using duplicate or triplicate injections and programmed methods. For all experiments phosphate buffered saline (PBS) at pH 7.4 and pH 6.0 with 0.01% (v/v) Tween20 and 0.05% (w/v) azide was used as running buffer. The chip was regenerated between injection cycles with two 10  $\mu$ l injections of 0.15M NaCl, 0.1M glycine pH 2.8 or 2.3 buffer. Equilibrium dissociation constants were determined using a 1:1 interaction model and custom written software SPRTTool ([www4.utsouthwestern.edu/wardlab/sprtool.asp](http://www4.utsouthwestern.edu/wardlab/sprtool.asp)).<sup>7</sup>

For competition binding assays, uncomplexed IL-6 at a concentration of 80 nM or in the presence of a 10-fold molar excess of antibody (0218, 0222, VH4 and VH9) was injected over immobilized 0218 at a flow rate of 10  $\mu$ l/min. The running buffer and sensor chip regeneration procedure was as described above. Analyte injections were performed in duplicates to ensure that there was no significant loss of ligand activity during the course of the experiment.<sup>8</sup>

*Transfections and sample preparation for fixed and live cell microscopy:* Microvasculature-derived human endothelial cells (HMEC-1) were transiently co-transfected with human FcRn-GFP (FcRn tagged at the C-terminus with GFP) or human FcRn-Stop and human  $\beta_2$ -microglobulin ( $\beta_2m$ ).<sup>9,10</sup> FcRn-Stop was designed to express FcRn without any fluorescent protein tag. This expression construct was generated by using the FcRn gene as a template and the following primers in the PCR: 5' ATC AGG ATC CTC AGG CGG TGG CTG GAA TCA CAT TTA C 3' (to append a stop codon followed by *Bam*HI site at the 3' end of the FcRn gene) and 5' TCC ATG CGC CTG AAG GCC CGA 3' (bases 611-630 of FcRn gene). The PCR product was digested with *Bam*HI (FcRn has an internal *Bam*HI site at bases 763-768), and the resulting *Bam*HI fragment was used to replace the 3' end of the FcRn gene in a previously described FcRn-GFP construct.<sup>10</sup> A mutated variant of human FcRn that has similar interaction properties as mouse FcRn was used throughout these studies.<sup>6</sup>

Transfections were performed using Nucleofector technology (Catalog no. WPB-1003 KT, Lonza, Hopkinton, MA). Transfected cells were plated in phenol red-free HAM'S F-12K medium (Catalog no. D9811-14C, US Biological, Swampscott, MA) on micro-coverglasses (Catalog no. 72224-01, Electron Microscopy Sciences, Hatfield, PA). 18 hours post-transfection, cells were pulsed at pH 7.4 with a pre-incubated equimolar (1:1) mixture of IL-6 with anti-IL-6 antibodies (0.165  $\mu$ M for fixed cell microscopy and 1.32  $\mu$ M for live cell microscopy) at 37°C in a 5% CO<sub>2</sub> incubator for one hour. For fixed cell imaging experiments, pulsed cells were washed twice with ice cold PBS and fixed by incubation in 1.7% paraformaldehyde (Catalog no. 19200, Electron Microscopy Sciences, Hatfield, PA) (w/v) with 0.025% (v/v) glutaraldehyde (Catalog no. G-5882, Sigma, St. Louis, MO) on ice for 10 minutes. For live cell imaging, pulsed cells were initially washed with HAM'S F-12K medium (pH adjusted to 7.4), followed by addition of pre-warmed medium (pH adjusted to 7.4, medium incubated in 37°C and equilibrated with 5% CO<sub>2</sub>).

*Microscopy image acquisition and analysis:* For fixed cell imaging, cells were imaged using a Zeiss Axiovert 200M inverted microscope equipped with a 63X, 1.4NA plan apochromat objective (Carl Zeiss, Thornwood, NJ), a 1.25X internal optovar and a cooled CCD camera (ORCA, Hamamatsu, Bridgewater, NJ). A mercury arc lamp was used as the excitation source and fluorescent filter sets for GFP (Catalog no. 41017), Alexa-555 (Catalog no. 41002b) and Cy5 (Catalog no. 41008) were used to acquire the images. All filter sets were purchased from Chroma Technology (Bellows Falls, VT).

Live cell imaging experiments were carried out using a custom built microscopy setup which has been described previously.<sup>9, 11</sup> Briefly, the microscope setup consists of a Zeiss Axiovert S100TV inverted microscope equipped with a 100X, 1.4NA plan apochromat objective (Carl Zeiss, Thornwood, NJ) and a cooled CCD camera (ORCA-ER or C8484-05; Hamamatsu, Bridgewater, NJ). The cell sample was excited by one or more of the following laser lines: 488 nm Argon-ion laser (Laser Physics, West Jordan, UT), 543 nm solid state laser (Opto Engine LLC, Midvale, UT) and a 633 nm Helium-Neon laser (JDS Uniphase, Milpitas, CA). The laser illumination of the sample was controlled through mechanical shutters. The laser lines were reflected onto the sample with a dichroic mirror (z488/543/633) and the emitted fluorescence was collected through the bottom port of the microscope. Emission filters specific for GFP (Catalog no. HQ525/50m), Alexa-555 (Catalog no. HQ590/50m) and Cy5 (Catalog no. HQ690/90m) were used to collect the fluorescence signal and were mounted in a motorized filter wheel (Ludl, Hawthorne, NY) which was positioned between the camera and the bottom port of the microscope. During imaging, an objective warmer was used to maintain the temperature of the cell sample at 37°C. The exposure time for each fluorophore was 200 ms, and a set of images were acquired every one second. Image acquisition and synchronization of shutters and filter wheel were performed through custom software written in the C programming language.

Acquired data was analyzed using MIATool ([www4.utsouthwestern.edu/wardlab/miatool.asp](http://www4.utsouthwestern.edu/wardlab/miatool.asp)). Events of interest (IgG or IgG/IL-6 sorting events) were manually identified and were selected for further analysis.<sup>12</sup> For display purposes, the intensities of the images were linearly adjusted to enable visualization of the sorting/trafficking events. Fluorescence intensity plots were generated by subtracting the background fluorescence intensity from the signal in regions of interest.

*Pharmacokinetic analyses:* 6-8 week old female CD-1 mice were obtained from Harlan Laboratories (Indianapolis, IN) and allowed to acclimate for one week prior to use in experiments. All studies performed on mice were approved by the MedImmune Institutional Animal Care and Use Committee (IACUC). 6  $\mu\text{g}$  of recombinant human IL-6 (R&D systems) was pre-incubated for 30 minutes with 221.67  $\mu\text{g}$  of 0222, 0218, or VH4. Mice were injected intravenously (i.v.) via the lateral tail vein with a total volume of 200  $\mu\text{l}$  protein. 12 mice per group were used and serum samples were collected by retro-orbital bleeding from 3 mice per group for each time point post-injection (5, 15, 30, 60 and 120 minutes) to comply with IACUC regulations. Concentrations of human IL-6 in the serum samples were determined using Human IL-6 Quantikine ELISA Kit (R&D Systems) according to the manufacturer's protocol. Plates were read at OD 450 nm using a Molecular Devices VMAX plate reader (Sunnyvale, CA). Data are plotted as concentration of IL-6 vs. time, rather than % injected dose, since this display better represents the rapid clearance of IL-6 (e.g. 5 minute time point, Figure 5) to be visualized. Statistical analyses were carried out using ANOVA in the statistics toolbox of MATLAB. For ANOVA, paired comparisons between different mouse groups were conducted using the Tukey-Kramer test at a 95% confidence level. *P* values of less than 0.05 for Student's *t*-test were taken to be significant.

*Molecular modeling and docking:* The homology model structure of the Fv fragment of the 0218 antibody was built using Discovery Studio 3.1 suite (DS 3.1) (Accelrys, San Diego, CA). A

BLAST search was performed against the Protein databank (PDB) to identify homologs with high sequence homology with the VH and VL domains of 0218. A PSI-BLAST search was performed against the PDB to identify a framework template for the relative spatial orientation of the VH and VL domains. Five hundred models of the Fv domain of 0218 were constructed using MODELLER implemented in DS3.1 with the identified templates in the PDB. The top scoring model with the lowest probability density function (PDF) energy was selected for CDR loop refinement. Only CDR2 and CDR3 of VH were selected for refinement using the template based approach since the templates found from the initial BLAST search provided sufficiently high homology for the other 4 CDRs. Fifty loop models for CDR2 and 3 were constructed and the conformation with the lowest PDF energy was selected for each CDR. High homology templates from the PDB were identified for modeling: VL template (2CMR, 100% identity), VH template (3EOT, 92% identity excluding CDR2 and 3), and VL/VH interface template (3G6J, 87% identity). The CDR2 and 3 of VH were refined using CDR loop templates of 71% identity for CDR2H and 50% identity for CDR3H. The quality of the model was validated using Profiles 3D and Ramachandran plots of DS 3.1.

ZDOCK was used to dock the crystal structure of IL-6 on to the modeled 0218 Fv tertiary structure. The coordinates of IL-6 (PDB ID 1p9m) were prepared for docking using the protein preparation tool in DS. The CHARMM forcefield was applied throughout the simulation. The docking was performed at a 6° angular step size and clustered for the top 200 poses. The docking results were processed according to the effects of histidine scanning mutagenesis of the CDR3s of the VH and VL domains on IL-6 binding and further optimized using RDOCK. The top 200 poses in the largest clusters were manually analyzed by examining the interface between IL-6 and 0218 Fv. Incorporation of the effects of histidine scanning on IL-6 binding combined with the ability of 0218 to inhibit the IL-6:IL-6R interaction resulted in a 0218:IL-6 model with the top ranking score (Supplementary Figure 7).

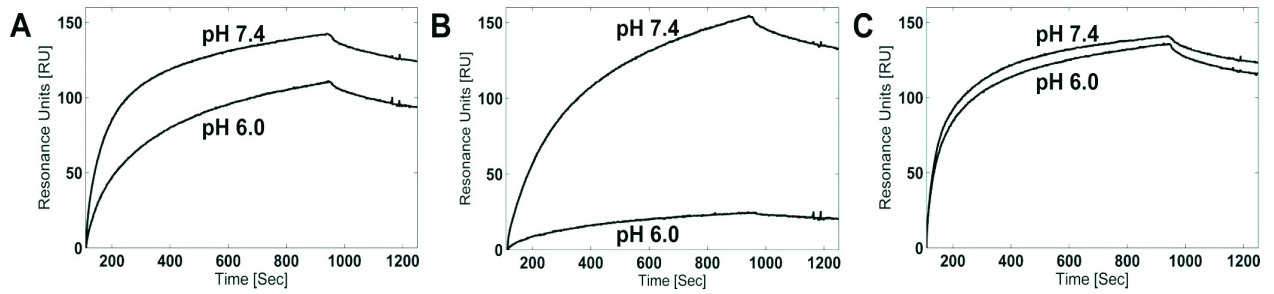
### Heavy chain variable domain

```
0218 EVQLVQSGGGVVPQPGESLRLSCAASGFTFSSYSMNWVRQAPGKLEWVSVIYSGGSTYYADSVKGRFTISRDNISKNTLYLQMNSLRAEDTAVYYCAREVYDSSGGYDDAFDIWGRGTMVTVSS
0218-VH1 -----H-----
0218-VH2 -----H-----
0218-VH3 -----H-----
0218-VH4 -----H-----
0218-VH5 -----H-----
0218-VH6 -----H-----
0218-VH7 -----H-----
0218-VH8 -----H-----
0218-VH9 -----H-----
0218-VH10 -----H-----
0218-VH11 -----H-----
0218-VH12 -----H-----
0218-VH13 -----H-----
0218-VH14 -----H-----
```

### Light chain variable domain

```
0218 DIQMTQSPSTLSASIGDRVITTCRASEGIYHWLAWYQQKPKAPKLLIYKASSLASGAPSRFSGSGSGTDFTLTISSLQPDDEATYYCQQYSNYPLTFGGGTKLEIK
0218-VL1 -----H-----
0218-VL2 -----H-----
0218-VL3 -----H-----
0218-VL4 -----H-----
0218-VL5 -----H-----
0218-VL6 -----H-----
0218-VL7 -----H-----
0218-VL8 -----H-----
0218-VL9 -----H-----
```

Supplementary Figure 1: Histidine scanning mutations of light and heavy chain CDR3s of antibody 0218.



Supplementary Figure 2: The anti-IL-6 antibodies bind to IL-6 with different pH dependencies.

Surface plasmon resonance (SPR) analyses of the interaction of *A*, 0218, *B*, VH4 and *C*, 0222 with IL-6. IL-6 at a concentration of 80 nM was injected over immobilized antibodies at pH 7.4 and pH 6.0 and representative sensorgrams are shown.

## Heavy chain variable domain

	FW-1	CDR-1	FW-2	CDR-2				
0222	EVQLLES	GGGLVQP	GGSLRLS	CAASGFTFSSY	AMSWVRQ	APGKGLEW	VSAISG	SGGSTYY
0218	EVQLVQ	SGGGVVQ	PGESLRLS	CAASGFTFSSYS	MNWVRQ	APGKGLEW	SVIY-	SGGSTYY
VH4	EVQLVQ	SGGGVVQ	PGESLRLS	CAASGFTFSSYS	MNWVRQ	APGKGLEW	SVIY-	SGGSTYY

	FW-3	CDR-3	FW-4			
0222	ADSVKGRFTISRDN	SKNTLYLQ	MNSLRAEDTAVYY	CARREFG----	ELFFDSWGRG	TLVT
0218	ADSVKGRFTISRDN	SKNTLYLQ	MNSLRAEDTAVYY	CAREVYD	SSGYDDAFDI	WGRGTMVT
VH4	ADSVKGRFTISRDN	SKNTLYLQ	MNSLRAEDTAVYY	CAREVYH	SSGYDDAFDI	WGRGTMVT

0222	VSS
0218	VSS
VH4	VSS

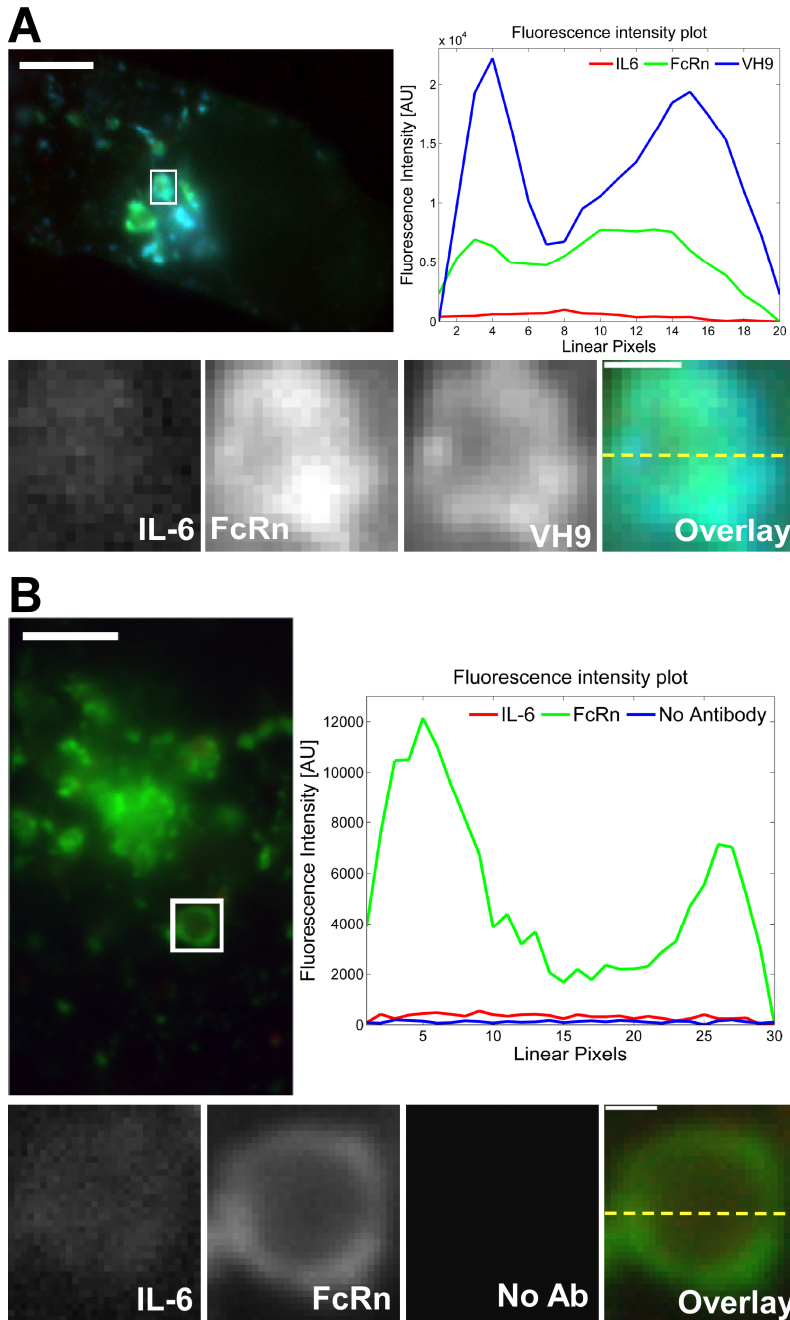
## Light chain variable domain

	FW-1	CDR-1	FW-2	CDR-2					
0222	QSVLTQ	PPS-VSG	APGQRVTI	SCTGSSSN	IGAGYDV	HVYQQ	LPGTAP	KLLIYG	NSN
0218/VH4	DIQMTQ	SPSTLS	SASIGDR	VTITCRAS---	EGIYH	LAWYQ	KPGKAP	KLLIY	KASS

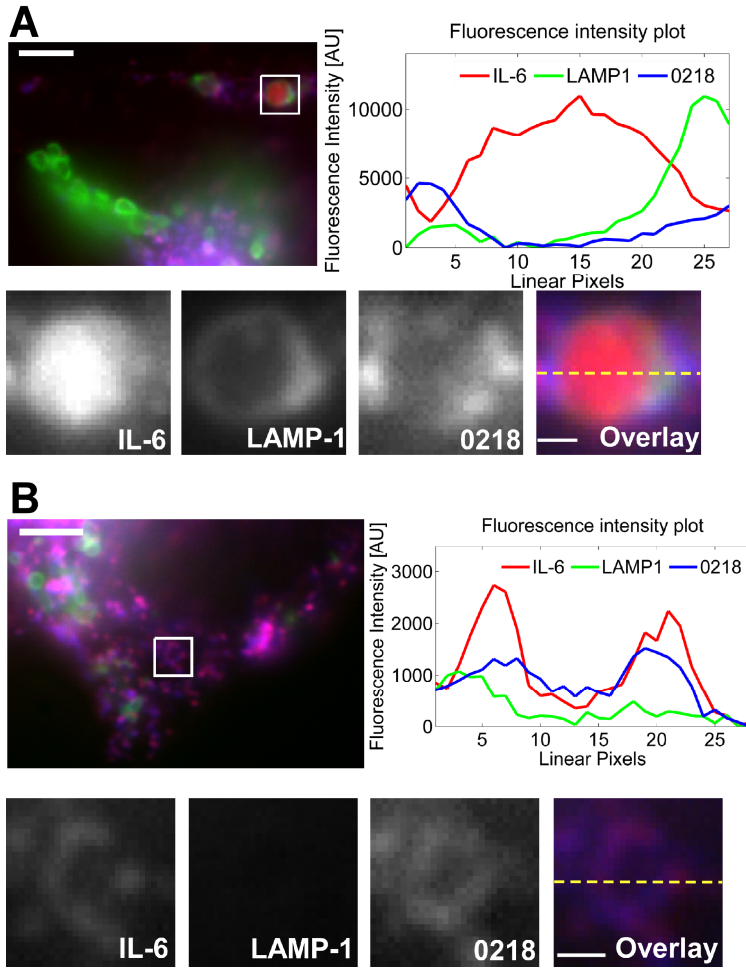
	FW-3	CDR-3	FW-4							
0222	RPSGVP	DRFSGS	KGTSAS	LAITGLQ	AEADYYC	QSYDTS	LSGWF	GGG	TKVTVL	
0218/VH4	LASGAP	SRFSGS	SGTDFT	LTISLQ	PDDFAT	YYCQ	YSN--	YPLTF	GGG	TKLEIK

Supplementary Figure 3: Sequence alignment of 0222, 0218, and VH4. Amino acid sequences of the VH and VL domain genes were aligned using T-Coffee.<sup>13</sup> The point mutation introduced in the CDR3 region of VH4 by histidine scanning mutagenesis is highlighted by a box.

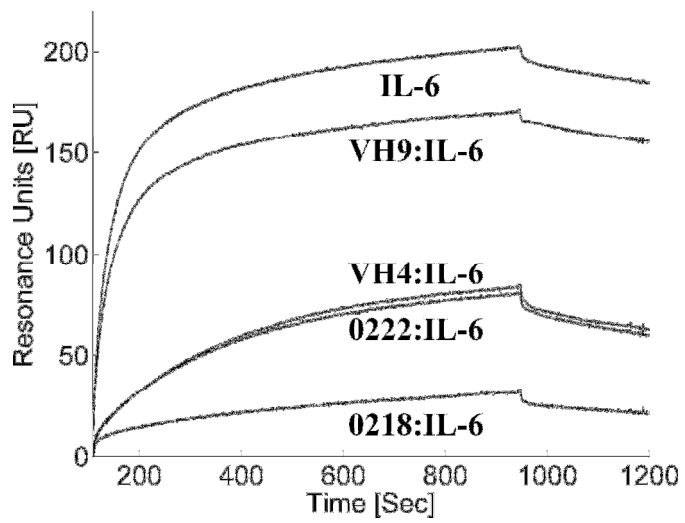


**Supplementary Figure 4:** Uncomplexed IL-6 accumulates to very low levels in cells. *A, B*, HMEC-1 cells were co-transfected with FcRn-GFP and  $\beta$ 2m. Transfected cells were pulsed with an equimolar ratio of IL-6 (labeled with Alexa-555) and Alexa-647 labeled antibody VH9 (*A*), or IL-6 alone (*B*) for 60 minutes, fixed and imaged. Images of representative cells are shown with

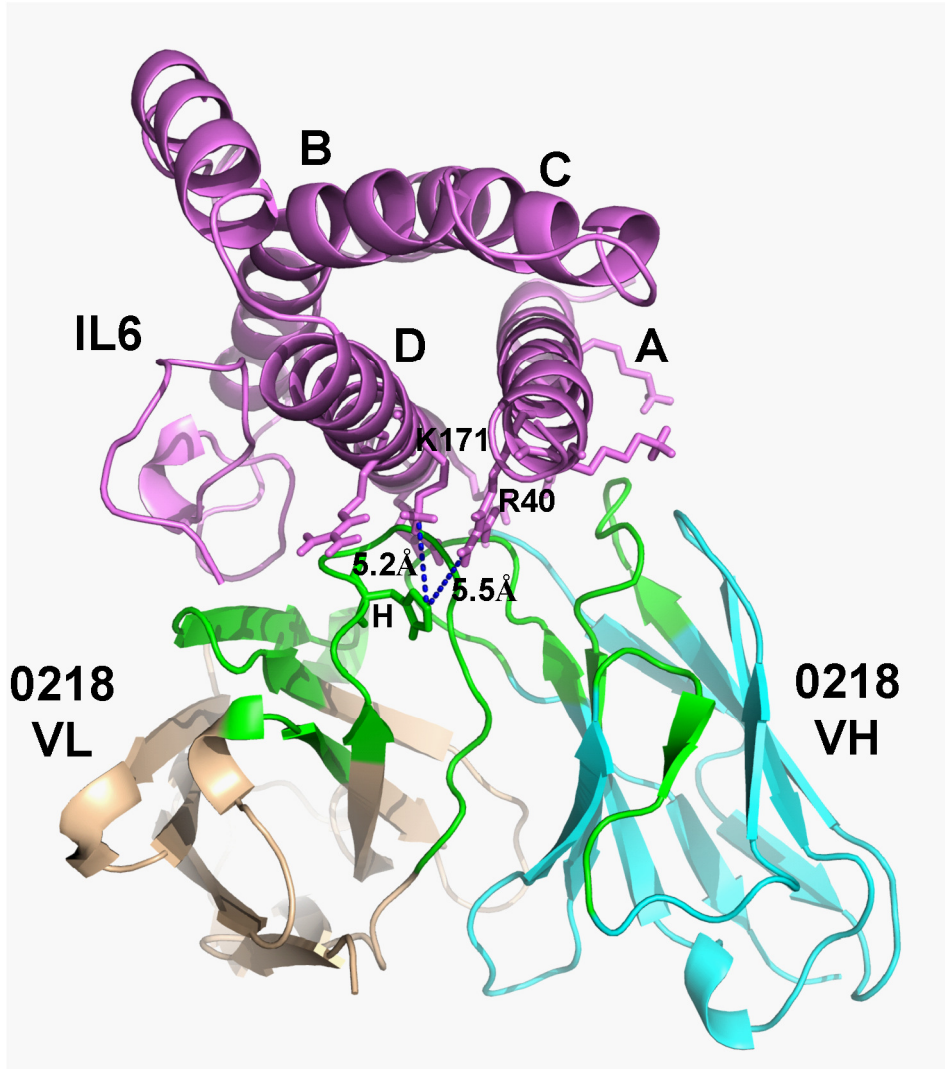
GFP, Alexa-647 and Alexa-555 pseudo-colored in green, blue and red, respectively. In each of *A*, and *B*, the endosome in the inset is cropped, expanded and presented as black and white images for the labeled proteins. In addition, the black and white images are shown as an overlay with the proteins represented by their pseudo-colors. Background-subtracted fluorescence intensities along the dotted lines in the overlays are shown in the fluorescence intensity plots. The scale bars for the complete cell images represent 6.4 and 4  $\mu\text{m}$  for panels *A* and *B*, respectively. For the cropped endosome scale bars represent 0.5 and 1.0  $\mu\text{m}$  for panels *A* and *B*, respectively.



**Supplementary Figure 5:** IL-6 dissociates from 0218 in late, but not early, endosomes. HMEC-1 cells were co-transfected with LAMP-1-GFP, FcRn-Stop and  $\beta$ 2m. Transfected cells were pulsed with an equimolar ratio of 0218 (labeled with Atto-647) and IL-6 (labeled with Alexa-555) for 60 minutes, fixed and imaged. *A-B*, Images of representative cells are shown with GFP, Atto-647 and Alexa-555 pseudo-colored in green, blue and red, respectively. The endosome in the inset is cropped, expanded and presented as black and white images for each of IL-6, LAMP-1 and 0218. In addition, the black and white images are shown in an overlay with the proteins represented by their pseudo-colors. Background-subtracted fluorescence intensities along the dotted lines in the overlays are shown in the fluorescence intensity plots. The scale bars for the complete cell images and the cropped endosomes represent 4 and 0.5  $\mu$ m, respectively.



Supplementary Figure 6: 0218, VH4 and 0222 bind to the same or overlapping epitope of IL-6. SPR analyses of the interaction of IL-6, 0218:IL-6, 0222:IL-6, VH4:IL-6 and VH9:IL-6 with immobilized 0218. IL-6 was injected at a concentration of 80 nM either alone (upper trace) or in complex with a 10-fold molar excess of the indicated antibodies.



Supplementary Figure 7: Putative binding interaction between IL-6 and 0218. Ribbon representation of the docked complex between IL-6 and the homology model of the 0218 Fv fragment. The CDRs of 0218 are shown in green for both VH (wheat) and VL (cyan). The positively charged amino acids of IL-6 (purple) in the binding interface are represented by sticks. The mutated histidine residue of CDR3 (shown by stick representation) is at a distance of  $\sim 5.5 \text{ \AA}$  from residues R40 and K171 of IL-6.

## **SI Movies**

Supplementary Movie 1: The movie corresponds to Figure 2A. Arrows indicate events of interest.

Movie plays at 0.5 x acquisition speed. Scale bar represents 1  $\mu\text{m}$ .

Supplementary Movie 2: The movie corresponds to Figure 2B. Arrows indicate events of interest.

Movie plays at 0.5 x acquisition speed. Scale bar represents 1  $\mu\text{m}$ .

Supplementary Movie 3: The movie corresponds to Figure 2C. Arrows indicate events of interest.

Movie plays at 0.5 x acquisition speed. Scale bar represents 1  $\mu\text{m}$ .

Supplementary Movie 4: The movie corresponds to Figure 3B. Arrows indicate events of interest.

Movie plays at 0.5 x acquisition speed. Scale represents 1  $\mu\text{m}$ .

## SI References

1. Vaughan TJ, Williams AJ, Pritchard K, Osbourn JK, Pope AR, Earnshaw JC, et al. Human antibodies with sub-nanomolar affinities isolated from a large non-immunized phage display library. *Nat Biotechnol* 1996; 14:309-14.
2. Lloyd C, Lowe D, Edwards B, Welsh F, Dilks T, Hardman C, et al. Modelling the human immune response: performance of a 1011 human antibody repertoire against a broad panel of therapeutically relevant antigens. *Protein Eng Des Sel* 2009; 22:159-68.
3. Finch DK, Sleeman MA, Moisan J, Ferraro F, Botterell S, Campbell J, et al. Whole-molecule antibody engineering: generation of a high-affinity anti-IL-6 antibody with extended pharmacokinetics. *J Mol Biology* 2011; 411:791-807.
4. Osbourn JK, McCafferty J, Derbyshire EJ, Waibel R, Chester K, Boxer G, et al. Isolation of a panel of human anti-CEA single chain Fv from a large phage display library. *Tumor Targeting* 1999; 4:150-7.
5. Kabat EA, Wu, T.T., Bilofsky, H., Reid-Miller, M., Perry. H. *Sequence of Proteins of Immunological Interest*. Bethesda: National Institute of Health, 1992.
6. Zhou J, Mateos F, Ober RJ, Ward ES. Conferring the binding properties of the mouse MHC class I-related receptor, FcRn, onto the human ortholog by sequential rounds of site-directed mutagenesis. *J Mol Biol* 2005; 345:1071-81.
7. Ober RJ, Caves J, Ward ES. Analysis of exponential data using a noniterative technique: application to surface plasmon experiments. *Anal Biochem* 2003; 312:57-65.
8. Ober RJ, Ward ES. Compensation for loss of ligand activity in surface plasmon resonance experiments. *Anal Biochem* 2002; 306:228-36.
9. Ober RJ, Martinez C, Vaccaro C, Zhou J, Ward ES. Visualizing the site and dynamics of IgG salvage by the MHC class I-related receptor, FcRn. *J Immunol* 2004; 172:2021-9.

10. Prabhat P, Gan Z, Chao J, Ram S, Vaccaro C, Gibbons S, et al. Elucidation of intracellular recycling pathways leading to exocytosis of the Fc receptor, FcRn, by using multifocal plane microscopy. *Proc Natl Acad Sci U.S.A* 2007; 104:5889-94.
11. Ward ES, Ober RJ. Chapter 4: Multitasking by exploitation of intracellular transport functions: the many faces of FcRn. *Adv Immunol* 2009; 103:77-115.
12. Chao J, Ward ES, Ober RJ. A software framework for the analysis of complex microscopy image data. *IEEE Trans Inf Technol Biomed* 2010; 14:1075-87.
13. Notredame C, Higgins DG, Heringa J. T-Coffee: A novel method for fast and accurate multiple sequence alignment. *J Mol Biol* 2000; 302:205-17.